

Semirelativistic approximation to the $\gamma^*N \rightarrow N(1520)$ and $\gamma^*N \rightarrow N(1535)$ transition form factors

G. Ramalho

*International Institute of Physics, Federal University of Rio Grande do Norte,
Campus Universitário – Lagoa Nova, CP. 1613, Natal, Rio Grande do Norte 59078-970, Brazil*
(Dated: April 12, 2019)

The representation of the wave functions of the nucleon resonances within a relativistic framework is a complex task, particularly for resonances with negative parity. In a nonrelativistic framework the orthogonality between states can be imposed naturally. In a relativistic generalization, however, the derivation of the orthogonality condition between states can be problematic, particularly when the states have different masses. In this work we study the $N(1520)$ and $N(1535)$ states using a relativistic framework. We considered wave functions derived in previous works, but impose the orthogonality between the nucleon and resonance states using the proprieties of the nucleon, ignoring the difference of masses between the states (semirelativistic approximation). The $N(1520)$ and $N(1535)$ wave functions are then defined without any adjustable parameters and are used to make predictions for the valence quark contributions to the transition form factors. The predictions compare well with the data particularly for high momentum transfer, where the dominance of the quark degrees of freedom is expected.

I. INTRODUCTION

In the last century we had learned that the hadrons, including the nucleon (N) and the nucleon excitations (N^*) are not pointlike particles and have their own internal structure. The structure of those states is the result of the internal constituents, quarks and gluons, and the interactions ruled by Quantum Chromodynamics (QCD). In the last decades experimental facilities such as Jefferson Lab (JLab), MAMI (Mainz) and MIT-Bates accumulated information (data) about the electromagnetic structure of the nucleon resonances, parametrized in terms of structure form factors for masses up to 3 GeV [1, 2].

Several theoretical models had been proposed to interpret the nucleon resonance spectrum and the information associated with their internal structure [1–3]. Different models provide different parametrizations of the internal structure in terms of the internal degrees of freedom. Some of the more successful models are the constituent quark models (CQM) based on nonrelativistic kinematics like the Karl-Isgur model [3, 4] and the Light Front quark models (LFQM) defined in the infinite momentum frame [5–7]. In those extreme cases, nonrelativistic models or LFQM, the kinematics is simplified. In general, however, the transition between the nonrelativistic and the relativistic regimes is not a trivial task.

In this work we discuss the $\gamma^*N \rightarrow N^*$ transition, form factors for N^* negative parity states. The definition of the wave functions of the nucleon (mass M_N) and a nucleon excitation (mass M_R), in terms of the internal quark degrees of freedom can be done first in the rest frame of the particle, and extended later for a moving frame, using a Lorentz transformation. In a nonrelativistic framework the mass and energy of the state are not

relevant for the definition of the states. Moreover, the orthogonality between the nucleon and N^* is ensured, since the wave functions are independent of their masses. To understand the complexity of the generalization of the orthogonality condition from a nonrelativistic framework for a relativistic framework, we consider the example of charge transition, J^0 , between a spin 1/2 negative parity state (R) and the nucleon (N). The projection of J^0 in the nucleon and N^* states at zero square momentum transfer ($q^2 = 0$) is proportional to the overlap between wave functions. One can show that in a relativistic framework the overlap is proportional to $\bar{u}_R \gamma_5 u_N$ [8]. In a framework where we can neglect the mass difference between the states¹ we obtain $\bar{u}_R \gamma_5 u_N = 0$, for the case where N and R have the same momentum ($q^2 = 0$). We then conclude that in the nonrelativistic limit the orthogonality between states is naturally ensured. In a relativistic framework the imposition of the orthogonality condition is more complex, since the nucleon and the resonance R cannot be at rest in the same frame, and the boost changes the proprieties of the states. As a consequence, states that are orthogonal when the mass difference can be neglected may not be orthogonal when the mass difference is taken into account.

The problem about how to define a wave function of a nucleon excitation that generalizes the nonrelativistic structure of the state and it is also orthogonal to the nucleon was already discussed in the context of the covariant spectator quark model for the negative parity res-

¹ The nonrelativistic limit can also be defined as the equal mass limit ($M_R = M_N$) or as the heavy baryon limit, when the terms on $(M_R - M_N)/M_N$ can be neglected.

onances, $N(1520)$ and $N(1535)$ [8–10]. The solution at the time was to define the radial wave functions for the N^* states in order to ensure the orthogonality with the nucleon state. The price to pay was the introduction of a new momentum scale parameter in the radial wave functions, to be determined by the phenomenology.

In this work we discuss an alternative approach. Instead of focus on the necessity of imposing the orthogonality between states, we assume that the mass difference is not the more relevant factor and treat the two states as different states with the same mass M , defined by the average $M = \frac{1}{2}(M_N + M_R)$. We call this approximation the semirelativistic approximation, since we keep features of the nonrelativistic regime (no mass dependence) and maintain a covariant description of the states.

The great advantage of the previous assumption is that, as explained in detail later, one can relate the radial wave function of the resonance R with the radial wave function of the nucleon, increasing the predictive power of the model. Later on, we discuss how to calculate the transition amplitudes using the form factors defined in the equal mass limit.

In this work we will show that, the results from the semirelativistic approximation compare well with $\gamma^*N \rightarrow N(1520)$ and $\gamma^*N \rightarrow N(1535)$ form factor data [11–17], particularly for large square momentum transfer ($Q^2 = -q^2$), and also with the estimates of the valence quark contributions to the transition form factors [18, 19]. At low Q^2 the agreement is not so good, since the meson cloud contributions are expected to be important and even dominant in some transitions [1, 2, 18, 20, 21].

This article is organized as follows: In Sec. II, we discuss the orthogonality between states and explain how the orthogonality can be imposed in a relativistic framework. In Sec. III, we present the formalism required to study the $\gamma^*N \rightarrow N(1520)$ and $\gamma^*N \rightarrow N(1535)$ transitions and the relations between electromagnetic currents, helicity amplitudes and form factors. Next, in Sec. IV, we discuss the covariant spectator quark model and present the model predictions for the transitions under study. The results of the semirelativistic approximation are discussed in the Sec. V. Outlook and conclusions are presented in Sec. VI.

II. ORTHOGONALITY AND RELATIVITY

We discuss now the orthogonality between two states: the nucleon (N) and a nucleon excitation R . Since they represent different systems they should be represented by orthogonal wave functions, Ψ_N and Ψ_R , respectively. In a quark-diquark model one can represent those wave functions by $\Psi_N(P, k)$ and $\Psi_R(P, k)$, where P and k are respectively the baryon and the diquark momenta ($P - k$ is the momentum of the single quark). For simplicity we ignore other indices, like the angular momentum, the spin and isospin projections.

In a nonrelativistic framework, the orthogonality be-

tween the wave functions is ensured when the overlap between the two wave functions vanishes in the limit where both particles have zero three-momentum, $\mathbf{P} = \mathbf{0}$, which can be represented, ignoring the isospin effect for now, by the condition

$$\sum_{\Gamma} \int_k \Psi_R^\dagger(\bar{P}, k) \Psi_N(\bar{P}, k) = 0, \quad (2.1)$$

In the previous equation Γ is a diquark polarization index and $\bar{P} = (M, \mathbf{0})$ is the nucleon and R momenta (\bar{P} is used to label P in the limit $Q^2 = 0$). The mass/energy component was introduced to facilitate the relativistic generalization, but it is irrelevant for the present discussion, since in the nonrelativistic limit the wave functions are defined only as function of the three-momentum. An important point about the Eq. (2.1) is that it is defined for the zero three-momentum transfer ($|\mathbf{q}| = 0$), since both states wave the same three-momentum $\mathbf{P} = \mathbf{0}$. In a covariant language we can write $Q^2 = -|\mathbf{q}|^2 = 0$, since we assumed that the energy is irrelevant for transitions at $|\mathbf{q}|^2 = 0$.

The question now is how to generalize the condition (2.1), defined for $Q^2 = 0$, to the relativistic case, particularly to the unequal mass case. In the context of the covariant spectator quark model [22–24], the problem was already discussed for several baryon systems [8, 9, 25–27]. In that formalism the relativistic generalization of Eq. (2.1) is

$$\sum_{\Gamma} \int_k \Psi_R^\dagger(\bar{P}_+, k) \Psi_N(\bar{P}_-, k) = 0, \quad (2.2)$$

where \bar{P}_+ and \bar{P}_- represent the resonance R and the nucleon momenta, respectively, in the case $Q^2 = 0$. Taking for instance the R rest frame, one has, assuming that the momentum transfer \mathbf{q} is along the z -axis:

$$\begin{aligned} \bar{P}_+ &= (M_R, 0, 0, 0), \\ \bar{P}_- &= (E_N, 0, 0, -|\mathbf{q}|), \end{aligned} \quad (2.3)$$

where $E_N = \frac{M_R^2 + M_N^2}{2M_R}$ and $|\mathbf{q}| = \frac{M_R^2 - M_N^2}{2M_R}$.

From the previous relations we conclude that in the case $Q^2 = 0$, we cannot have R and N at rest at the same time (in the same frame) unless the $M_R = M_N$. Thus, in the conditions of Eqs. (2.3), the resonance R is at rest but the nucleon is not at rest ($|\mathbf{q}| \neq 0$).

The discussion about the orthogonality between states that are not defined in the rest frame is more complex, and has consequences in the calculation of the transition form factors in the limit $Q^2 = 0$. We can illustrate the problem looking for the magnetic form factor G_M for the $\gamma^*N \rightarrow N(1520)$ transition. As discussed in Ref. [9], the orthogonality condition implies that $G_M(0) \propto \mathcal{I}_R(0)$, where $\mathcal{I}_R(Q^2)$ is a integral defined by the overlap between the nucleon and R radial wave functions (details can be found in Ref. [9]). Since the orthogonality condition between states is equivalent to $\mathcal{I}_R(0) = 0$ [9], one obtains

$G_M(0) = 0$, in contradiction with the experimental result $G_M(0) = -0.393 \pm 0.044$ [11].

In the framework of the covariant spectator quark model, we can prove that the orthogonality condition (2.2) for the states $R = N(1520)$, $N(1535)$ is equivalent to [8, 9]

$$\mathcal{I}_R(0) = \int_k \frac{k_z}{|\mathbf{k}|} \psi_R(\bar{P}_+, k) \psi_N(\bar{P}_-, k) = 0, \quad (2.4)$$

where ψ_R and ψ_N are radial wave functions from R and N , respectively (real functions of $(\bar{P}_\pm - k)^2$). The integral $\mathcal{I}_R(0)$ is defined in Eq. (2.4) in the R rest frame, by simplicity. The general expression can be found in Refs. [8, 9].

In the Sec. IV, we will present the results for the $\gamma^* N \rightarrow N(1520)$ and $\gamma^* N \rightarrow N(1535)$ form factors and the connection with the helicity amplitudes within the covariant spectator quark model.

For the $\gamma^* N \rightarrow N(1520)$ one has 3 independent form factors G_i ($i = 1, 2, 3$), with the form [9]

$$G_i(Q^2) \propto \frac{\mathcal{I}_R(Q^2)}{|\mathbf{q}|}, \quad (2.5)$$

when $Q^2 \rightarrow 0$. In the case $\frac{\mathcal{I}_R(Q^2)}{|\mathbf{q}|} \rightarrow \text{const}$, one has finite contributions for the transverse amplitudes $A_{1/2}(0)$ and $A_{3/2}(0)$, consistently with the experimental data.

As for the $\gamma^* N \rightarrow N(1535)$ transition, we conclude that the two independent form factors F_i^* ($i = 1, 2$) can be represented as [8]

$$F_i^*(Q^2) \propto \mathcal{I}_R(Q^2) \quad (2.6)$$

when $Q^2 \rightarrow 0$. In addition, it can be shown that $\mathcal{I}_R \propto |\mathbf{q}|$ when the nucleon and the $N(1535)$ states are described by the same radial wave function [8]. As a consequence of Eq. (2.6), one obtains $F_1^*(0) = 0$, automatically in the limit $|\mathbf{q}| \rightarrow 0$.

The problem associated with the results from the $\gamma^* N \rightarrow N(1520)$ and $\gamma^* N \rightarrow N(1535)$ form factors given by Eqs. (2.5) and (2.6) is they are finite only in the case $|\mathbf{q}| \rightarrow 0$ when $Q^2 = 0$, which is inconsistent with $|\mathbf{q}| = \frac{M_R^2 - M_N^2}{2M_R} \neq 0$, unless $M_R = M_N$.

In previous works [8, 9], we developed models that or violate the orthogonality condition (2.4) as for the $\gamma^* N \rightarrow N(1535)$ transition [8], or are consistent with the orthogonality condition, but failed to describe the low Q^2 data, as for the $\gamma^* N \rightarrow N(1535)$ transition [9].

In the present work, we consider an alternative approach that tries to achieve two goals. For one side we want to keep the nice analytic proprieties of the form factors in the case $M_R = M_N$, which are spoiled in the relativistic generalization of wave function in the case $M_R \neq M_N$. For another side, we want to describe the experimental helicity amplitudes which are defined only in the case $M_R \neq M_N$. With those two ideas in mind we consider the following approximation: we assume that

both states, the nucleon and the resonance R are states with the same mass, given by the average between the two physical masses

$$M = \frac{1}{2}(M_R + M_N). \quad (2.7)$$

With this choice, the orthogonality condition (2.4) is automatically verified if ψ_R is defined as ψ_N . In that case the product $\psi_R(\bar{P}_+, k) \psi_N(\bar{P}_-, k)$ is symmetric in the angular variables when $|\mathbf{q}| = 0$, therefore the integral in k_z vanishes.

Since this approximation mimics the nonrelativistic limit when we ignore the mass differences, we refer this approximation as the semirelativistic approximation.

A nice consequence of the semirelativistic approach is that, since the R states are defined using the radial wave function of the nucleon (ψ_N) there are no adjustable parameters in the model. Therefore, the results of the present model are true predictions that can be compared with the experimental data.

III. FORMALISM

In this section we present the general definitions of the $\gamma^* N \rightarrow R$ helicity amplitudes at the final state (R) rest frame. Following the notation of previous works we use P_- for the initial state (nucleon) and P_+ for the final state (R). The momentum transfer is then $q = P_+ - P_-$. We use $Q^2 = -q^2$, that we relabel as the square momentum transfer. The transition current operator will be represented by J^μ , and is defined in units of the proton charge e . The explicit form of J^μ depends of the N and R states. To express the projection of J^μ in the states R and N we use the matrix element

$$J_{NR}^\mu \equiv \langle R | J^\mu | N \rangle. \quad (3.1)$$

Next, we present the general definition of the helicity amplitudes which are valid for any final state resonance with spin $1/2$ or $3/2$. Afterwards, we consider in particular the $\gamma^* N \rightarrow N(1520)$ and $\gamma^* N \rightarrow N(1535)$ transitions, and present the explicit expressions relations for the current and transition form factors.

Along this work we will use a common notation for the two transitions. The meaning of the index R , as in the function \mathcal{I}_R discussed previously, will depend of the transition under study. We will use also

$$\tau = \frac{Q^2}{(M_R + M_N)^2}, \quad (3.2)$$

for both transitions.

A. Helicity amplitudes

The electromagnetic transition $\gamma^* N \rightarrow R$, where R is state with angular momentum $J = \frac{1}{2}, \frac{3}{2}$ with positive or

negative parity ($J^P = \frac{1}{2}^\pm, \frac{3}{2}^\pm$) is characterized by the helicity amplitudes, functions of Q^2 , and defined at the R rest frame according to [1]:

$$A_{3/2} = \sqrt{\frac{2\pi\alpha}{K}} \langle R, S'_z = +\frac{3}{2} | \varepsilon_+ \cdot J | N, S_z = +\frac{1}{2} \rangle, \quad (3.3)$$

$$A_{1/2} = \sqrt{\frac{2\pi\alpha}{K}} \langle R, S'_z = +\frac{1}{2} | \varepsilon_+ \cdot J | N, S_z = -\frac{1}{2} \rangle, \quad (3.4)$$

$$S_{1/2} = \sqrt{\frac{2\pi\alpha}{K}} \langle R, S'_z = +\frac{1}{2} | \varepsilon_0 \cdot J | N, S_z = +\frac{1}{2} \rangle \frac{|\mathbf{q}|}{Q}. \quad (3.5)$$

In the previous equations S'_z (S_z) is the final (initial) spin projection, \mathbf{q} is the photon three-momentum in the R rest frame, $Q = \sqrt{Q^2}$, ε_λ^μ ($\lambda = 0, \pm 1$) is the photon polarization vector, $\alpha \simeq 1/137$ is the fine-structure constant and $K = \frac{M_R^2 - M^2}{2M_R}$. The amplitude $A_{3/2}$ is defined only for $J = \frac{3}{2}$ resonances.

At the R rest frame the magnitude of the photon three-momentum is $|\mathbf{q}|$, and reads

$$|\mathbf{q}| = \frac{\sqrt{Q_+^2 + Q_-^2}}{2M_R}, \quad (3.6)$$

where $Q_\pm^2 = (M_R \pm M_N)^2 + Q^2$. Note that when $Q^2 = 0$ one has $K = |\mathbf{q}| = \frac{M_R^2 - M_N^2}{2M_R}$ as mentioned above.

B. $\gamma^* N \rightarrow N(1520)$ transition

Because $N(1520)$ is a $J^P = \frac{3}{2}^-$ state, the $\gamma^* N \rightarrow N(1520)$ transition current can be represented as [1, 9]

$$J_{NR}^\mu = \bar{u}_\beta(P_+) \Gamma^{\beta\mu} u(P_-), \quad (3.7)$$

where u_β , u are, respectively, the Rarita-Schwinger and Dirac spinors. The operator $\Gamma^{\beta\mu}$ has the general Lorentz structure

$$\Gamma^{\beta\mu} = G_1 q^\beta \gamma^\mu + G_2 q^\beta P^\mu + G_3 q^\beta q^\mu - G_4 g^{\beta\mu}, \quad (3.8)$$

where $P = \frac{1}{2}(P_+ + P_-)$. The functions G_i ($i = 1, \dots, 4$) are form factor functions that depend on Q^2 , but only three of them are independent. From current conservation [9, 28] we conclude that

$$G_4 = (M_R - M_N)G_1 + \frac{1}{2}(M_R^2 - M_N^2)G_2 - Q^2 G_3. \quad (3.9)$$

Another useful combination of the form factors G_i ($i = 1, 2, 3$) is

$$g_C = 4M_R G_1 + (3M_R^2 + M_N^2 + Q^2)G_2 + 2(M_R^2 - M_N^2 - Q^2)G_3. \quad (3.10)$$

Using the previous form factors we can express the $\gamma^* N \rightarrow N(1520)$ helicity amplitudes defined by Eqs. (3.3)-(3.5) as [1, 9]

$$A_{1/2} = 2\mathcal{A}_R \left\{ G_4 - [(M_R - M_N)^2 + Q^2] \frac{G_1}{M_R} \right\} \quad (3.11)$$

$$A_{3/2} = 2\sqrt{3}\mathcal{A}_R G_4, \quad (3.12)$$

$$S_{1/2} = -\frac{1}{\sqrt{2}} \frac{|\mathbf{q}|}{M_R} \mathcal{A}_R g_C, \quad (3.13)$$

where $\mathcal{A}_R = \frac{e}{4} \sqrt{\frac{Q_+^2}{6M_N M_R K}}$.

For a discussion about the convenience of the combination of form factors G_1 , G_4 , g_C , see Ref. [9].

An alternative representation of the $\gamma^* N \rightarrow N(1520)$ electromagnetic structure are the so-called multipole electromagnetic form factors: the magnetic dipole (G_M), and the electric (G_E) and Coulomb (G_C) quadrupoles. Those form factors can be represented as [1, 9]

$$G_M = -\mathcal{R} [(M_R - M_N)^2 + Q^2] \frac{G_1}{M_R}, \quad (3.14)$$

$$G_E = -\mathcal{R} \left\{ 4G_4 - [(M_R - M_N)^2 + Q^2] \frac{G_1}{M_R} \right\}, \quad (3.15)$$

$$G_C = -\mathcal{R} g_C, \quad (3.16)$$

where $\mathcal{R} = \frac{1}{\sqrt{6}} \frac{M_N}{M_R - M_N}$.

C. $\gamma^* N \rightarrow N(1535)$ transition

We consider now the resonance $N(1535)$ which is a $J^P = \frac{1}{2}^-$ state. The $\gamma^* N \rightarrow N(1535)$ transition current can be represented as [1, 8, 29, 30]

$$J_{NR}^\mu = \bar{u}_R \left[F_1^* \left(\gamma^\mu - \frac{\not{q} \not{q}^\mu}{q^2} \right) + F_2^* \frac{i\sigma^{\mu\nu} q_\nu}{M_R + M_N} \right] \gamma_5 u, \quad (3.17)$$

where F_i^* ($i = 1, 2$) define the transition form factors and u_R , u are Dirac spinors associated with the R and the nucleon states, respectively. The analytic properties of the current (3.17) imply that $F_1^*(0) = 0$ [8].

The helicity amplitudes can be expressed in terms of the form factors using [1, 8, 31, 32]:

$$A_{1/2} = 2\mathcal{A}_R \left[F_1^* + \frac{M_R - M_N}{M_R + M_N} F_2^* \right] \quad (3.18)$$

$$S_{1/2} = -\sqrt{2}\mathcal{A}_R (M_R + M_N) \frac{|\mathbf{q}|}{Q^2} \times \left[\frac{M_R - M_N}{M_R + M_N} F_1^* - \tau F_2^* \right], \quad (3.19)$$

where $\mathcal{A}_R = \frac{e}{4} \sqrt{\frac{Q_+^2}{M_N M_R K}}$.

We discuss next the results of the covariant spectator quark model for the transitions under discussion.

IV. COVARIANT SPECTATOR QUARK MODEL

The covariant spectator quark model is derived from the formalism of the covariant spectator theory [33]. In the model, a baryon B is described as a three-constituent-quark system, where one quark is free to interact with the electromagnetic fields and the other quarks are on-mass-shell. Integrating over the on-mass-shell momenta, one can represent the quark pair as an on-mass-shell diquark with effective mass m_D , and the baryon as a quark-diquark system [2, 22–24]. The structure of the baryon is then described by a transition vertex between the three-quark bound state and a quark-diquark state, that describes effectively the confinement [22, 24].

The baryon wave function $\Psi_B(P, k)$ is derived from the transition vertex as a function of the baryon momentum P and the diquark momentum k , taking into account the properties of the baryon B , such as the spin and flavor. The wave functions are not determined by a dynamical equation but are instead built from the baryon internal symmetries, with the shape determined directly by experimental or lattice data for some ground state systems [2, 22, 34, 35]. The wave functions of the nucleon, $N(1520)$ and $N(1535)$ are discussed in Refs. [8, 9, 22].

The covariant spectator quark model was already applied to the nucleon [22, 23, 36, 37], several nucleon resonances [8–10, 25, 27], Δ resonances [10, 34, 35, 38–41], and other transitions between baryon states [24, 30, 42–44].

When the baryon wave functions are represented in terms of the single quark and quark-pair states, one can write the transition current in a relativistic impulse approximation as [22–24]

$$J_{NR}^\mu = 3 \sum_{\Gamma} \int_k \bar{\Psi}_R(P_+, k) j_q^\mu \Psi_N(P_-, k), \quad (4.1)$$

where j_q^μ is the quark current operator and Γ labels the scalar diquark and vectorial diquark (projections $\Lambda = 0, \pm$) polarizations. The factor 3 takes account of the contributions of all the quark-pairs by symmetry. The integration symbol represents the covariant integration for the diquark on-shell state $\int_k \equiv \int \frac{d^3\mathbf{k}}{(2\pi)^3(2E_D)}$, with $E_D = \sqrt{m_D^2 + \mathbf{k}^2}$.

The quark current operator can be written in terms of the Dirac (j_1) and Pauli (j_2) quark form factors [22, 24]:

$$j_q^\mu = j_1 \left(\gamma^\mu - \frac{\not{q} \not{q}^\mu}{q^2} \right) + j_2 \frac{i\sigma^{\mu\nu} q_\nu}{2M_N}. \quad (4.2)$$

The inclusion of the term $-\frac{\not{q} \not{q}^\mu}{q^2}$ associated with the Dirac component in inelastic reactions is equivalent to the Landau prescription for the current J^μ [45–47]. The term restores current conservation, but does not affect the results for the observables [45].

In the $SU(2)$ -flavor sector we can decompose ($i = 1, 2$)

$$j_i = \frac{1}{6} f_{i+} + \frac{1}{2} f_{i-} \tau_3. \quad (4.3)$$

where $f_{i\pm}(Q^2)$ are quark electromagnetic form factors, and normalized according to $f_{1\pm}(0) = 1$ and $f_{2\pm}(0) = \kappa_{\pm}$ (quark isoscalar/isovector anomalous magnetic moment). The quark electromagnetic form factors are written in terms of a vector meson dominance parametrization that simulates effectively the constituent quark internal structure due to the interactions with gluons and quark-antiquark polarization effects. The quark electromagnetic current was calibrated previously by the nucleon and decuplet baryon data [22, 24], and was also tested in the lattice regime for the nucleon elastic reaction as well as for the $\gamma N \rightarrow \Delta$ transition [24, 35, 40, 42]. Details can be found in Refs. [22, 24, 25, 27].

In the calculation of the transition current it is convenient to define the symmetric (S) and antisymmetric (A) projections of the isospin states ($i = 1, 2$)

$$j_i^S = \frac{1}{6} f_{i+} + \frac{1}{2} f_{i-} \tau_3 \quad (4.4)$$

$$j_i^A = \frac{1}{6} f_{i+} - \frac{1}{2} f_{i-} \tau_3. \quad (4.5)$$

The normalization of the states is imposed for $B = N, R$, through the condition

$$\sum_{\Gamma} \int_k \bar{\Psi}_B(\bar{P}, k) (3j_1) \gamma^0 \Psi_B(\bar{P}, k) = e_N, \quad (4.6)$$

where $\bar{P} = (M_B, 0, 0, 0)$ is the momentum at the rest frame, $e_N = \frac{1}{2}(1 + \tau_3)$ is the nucleon charge. In the previous equation $(3j_1)\gamma^0$ is the quark charge operator, with $j_1 = j_1(0)$. Assumed in Eq. (4.6) is the normalization of the radial wave function $\int_k |\psi_B(\bar{P}, k)|^2 = 1$.

The radial wave functions ψ_B ($B = N, R$) are represented in terms of the dimensionless variable [22]

$$\chi = \frac{(M_B - m_D)^2 - (P - k)^2}{M_B m_D}, \quad (4.7)$$

as

$$\psi_B(P, k) = \frac{N_0}{m_D(\beta_1 + \chi)(\beta_2 + \chi)}, \quad (4.8)$$

where N_0 is a normalization constant and the parameters $\beta_1 = 0.049$ and $\beta_2 = 0.717$ were determined by the model for the nucleon with a fit to the nucleon electromagnetic form factor data [22]. The relative sign of N_0 for the resonances $N(1520)$, $N(1535)$ is determined by the sign of the transition form factors [8, 9]. With the inclusion of the factor $1/m_D$ in the definition of the radial wave function (4.8), the diquark mass dependence scales out of in the integration ($k \rightarrow k/m_D$) and the form factors became independent of m_D [22, 24].

The orthogonality condition between the nucleon and R wave functions, now generalized with the effect of the isospin, is [8, 9]:

$$\sum_{\Gamma} \int_k \bar{\Psi}_R(\bar{P}_+, k) (3j_1) \gamma^0 \Psi_N(\bar{P}_-, k) = 0. \quad (4.9)$$

From the previous expression we can derive the orthogonality relation for the radial wave functions, given by Eq. (2.4) [8, 9].

For the calculation of the transition form factors it is convenient to define the overlap integral between the radial wave functions $\mathcal{I}_R(Q^2)$ as

$$\mathcal{I}_R(Q^2) = \int_k \frac{k_z}{|\mathbf{k}|} \psi_R(P_+, k) \psi_N(P_-, k), \quad (4.10)$$

The previous integral is represented in the R rest frame, where the form is simplified. The function $\mathcal{I}_R(Q^2)$ defines, however, an invariant integral than can be calculated in any frame. The discussion associated with the general form of the integral can be found in Refs. [8, 9]. In the limit $Q^2 = 0$, we recover the form of $\mathcal{I}_R(0)$ presented in Eq. (2.4). As discussed in Sec. II, $\mathcal{I}_R(0) = 0$, when ψ_R is defined as ψ_N ($\psi_R \equiv \psi_N$) and $M_R = M_N$.

A. $\gamma^* N \rightarrow N(1520)$ form factors

The expressions for the $\gamma^* N \rightarrow N(1520)$ transition form factors are [9]

$$G_1 = -\frac{3}{2\sqrt{2}|\mathbf{q}|} \times \left[\left(j_1^A + \frac{1}{3} j_1^S \right) + \frac{M_R + M_N}{2M_N} \left(j_2^A + \frac{1}{3} j_2^S \right) \right] \mathcal{I}_R, \quad (4.11)$$

$$G_2 = \frac{3}{2\sqrt{2}M_N|\mathbf{q}|} \times \left[j_2^A + \frac{1}{3} \frac{1-3\tau}{1+\tau} j_2^S + \frac{4}{3} \frac{2M_N}{M_R + M_N} \frac{1}{1+\tau} j_1^S \right] \mathcal{I}_R, \quad (4.12)$$

$$G_3 = -\frac{3}{2\sqrt{2}|\mathbf{q}|} \frac{M_R - M_N}{Q^2} \times \left[j_1^A + \frac{1}{3} \frac{\tau-3}{1+\tau} j_1^S + \frac{4}{3} \frac{M_R + M_N}{2M_N} \frac{\tau}{1+\tau} j_2^S \right] \mathcal{I}_R, \quad (4.13)$$

where τ is defined in Eq. (3.2).

Comparative with Ref. [9] we take the limit where the mixture angle θ_D is given by $\cos \theta_D \simeq 1$ (in most of the models $\cos \theta_D \simeq 0.99$ [48]).

When we calculate G_4 using (3.9), we obtain

$$G_4 = 0. \quad (4.14)$$

Thus, in the covariant spectator quark model one has, according to Eqs. (3.12), (3.14) and (3.15): $A_{3/2} \equiv 0$ and $G_E \equiv -G_M$ [9].

For the following discussion we note that the form factors G_i ($i = 1, 2, 3$) given by Eqs. (4.11)-(4.13) are proportional to the factor $\frac{\mathcal{I}_R(Q^2)}{|\mathbf{q}|}$.

The results (4.11)-(4.13) were derived in Ref. [9]. In that work ψ_R was parametrized in order to describe the

large Q^2 data (small meson cloud effects) and the orthogonality condition, $\mathcal{I}_R(0) = 0$. As a consequence the valence quark contributions for the form factors G_M , G_E and the amplitude $A_{1/2}$ vanishes at $Q^2 = 0$. This feature changes in the semirelativistic approximation, as we will show.

Another interesting propriety of the model is that the results for the form factors G_i imply that $A_{3/2} = 0$ for all values of Q^2 , which is in contradiction with the available experimental data. Our interpretation of this result is that the main contribution for the amplitude $A_{3/2}$ comes from the meson cloud effects. Most of the quark models predict small contributions for the amplitude $A_{3/2}$ [9, 10]. Estimates of the meson cloud contributions from the EBAC coupled-channel reaction model also support the idea that the meson cloud is the dominate effect in $A_{3/2}$ [18].

B. $\gamma^* N \rightarrow N(1535)$ form factors

The expressions for the $\gamma^* N \rightarrow N(1535)$ transition form factors are [9]

$$F_1^*(Q^2) = \frac{1}{2} (3j_1^S + j_1^A) \mathcal{I}_R, \quad (4.15)$$

$$F_2^*(Q^2) = -\frac{1}{2} (3j_2^S - j_2^A) \frac{M_R + M_N}{2M_N} \mathcal{I}_R. \quad (4.16)$$

In Ref. [8] we presented a model with $\mathcal{I}_R(0) \neq 0$. The consequence of $\mathcal{I}_R(0) \neq 0$ is that the nucleon and the resonance $N(1535)$ are not orthogonal. The results presented in Ref. [8] were based on an approximated orthogonality, and are valid only for large Q^2 ($Q^2 \gg K^2 \simeq 0.2 \text{ GeV}^2$). In the present work, within the semirelativistic approximation, the orthogonality is exact.

V. RESULTS IN THE SEMIRELATIVISTIC APPROXIMATION

We present now the results of the semirelativistic approximation for the $\gamma^* N \rightarrow N(1520)$ and the $\gamma^* N \rightarrow N(1535)$ transition form factors and respective helicity amplitudes.

The numerical results are compared to the data from CLAS single pion production [12] and double pion production [13, 14], MAID [15, 16], and Particle Data Group (PDG) ($Q^2 = 0$) [11]. For the $\gamma^* N \rightarrow N(1535)$ we show also results from JLab/Hall C [17] for the amplitude $A_{1/2}$.

A. $\gamma^* N \rightarrow N(1520)$ transition

The elementary form factors G_i ($i = 1, 2, 3$) for the $\gamma^* N \rightarrow N(1520)$ transition determined by the covariant spectator quark model are given by Eqs. (4.11)-(4.13).

Using those expressions for G_i we can evaluate the helicity amplitudes $A_{1/2}$, $A_{3/2}$, $S_{1/2}$ and the multipole form factors G_M , G_E and G_C .

In the semirelativistic approximation we can evaluate G_1 , G_2 , G_3 , in the limit $M_R = M_N$, using

$$\frac{M_R + M_N}{2M_N} \rightarrow 1 \quad (5.1)$$

$$|\mathbf{q}| \rightarrow Q\sqrt{1+\tau}, \quad (5.2)$$

and replacing also $M_N \rightarrow M$ in G_2 . A special care is necessary for the function G_3 , since it includes a factor $(M_R - M_N)/Q^2$. There is therefore the possibility of a singularity at $Q^2 = 0$. This singularity is only apparent as we explain next.

We start noticing that G_3 appears only in the function g_C given by Eq. (3.10), which can be expressed, in the limit $M_R = M_N$, as

$$g_C = 4MG_1 + (4M^2 + Q^2)G_2 - 2Q^2G_3. \quad (5.3)$$

Since the factor $1/Q^2$ on G_3 is canceled by the factor Q^2 , the limit $M_R = M_N$ can be performed obtaining $Q^2G_3 \rightarrow 0$ in the equal mass limit.

Note also that in G_4 , we can drop the term Q^2G_3 . We then conclude that in the limit $M_R = M_N$ all terms in G_4 vanish [see Eq. (3.9)].

We recall, from the previous section, that, the form factors G_i are proportional to $\frac{\mathcal{I}_R(Q^2)}{|\mathbf{q}|}$. Since $\mathcal{I}_R(Q^2) \propto |\mathbf{q}|$ near $Q^2 = 0$, when N and R are defined by the same radial wave function [8], in the approximation $M_R = M_N$, we ensure the orthogonality between the nucleon and resonance states, $\mathcal{I}_R(0) = 0$, and obtain also finite results at $Q^2 = 0$ ($\mathcal{I}_R(0)/|\mathbf{q}| \neq 0$).

In order to obtain the results in the semirelativistic approximation we calculate G_i ($i = 1, 2, 3$), G_4 , g_C in the limit $M_R = M_N$, and then use the relations (3.11)-(3.13), (3.14)-(3.16) to calculate the helicity amplitudes and the form factors G_M , G_E and G_C .

The conversion between G_1 , G_4 , g_C into helicity amplitudes and multipole form factors using coefficients dependent on the masses M_R and M_N is necessary, because the helicity amplitudes and G_M , G_E and G_C are only strictly defined in the case $M_R \neq M_N$. At the end we present also the results in the extreme limit, when we ignore all mass differences, except for the factors \mathcal{A}_R or \mathcal{R} .

1. Comparison with the data

The results of the semirelativistic approach (thick solid line) for the helicity amplitudes are present in the Fig. 1. The CLAS data [12–14] are represented by the full circles. For a cleaner comparison, we replace the MAID data by the MAID parametrization of the data [16] (thin solid line). Notice the deviation between the MAID and the CLAS data for the amplitudes $A_{1/2}$ and $S_{1/2}$. The points represented by the diamonds are discussed later.

It is interesting to see in the figure that, the semirelativistic approximation describes very well the high Q^2 CLAS data for the amplitudes $A_{1/2}$ and $S_{1/2}$. As for the $A_{3/2}$, as discussed already, the model predicts $A_{3/2} \equiv 0$.

The corresponding results for the form factors G_M , G_E and G_C are presented in Fig. 2, with the same labeling. The differences between the CLAS and MAID data are obvious for G_M and G_C . It is interesting to note in this case, that, although the semirelativistic approximation fail to describe the G_E data at low Q^2 , it approaches the data for $Q^2 > 3 \text{ GeV}^2$.

Overall it is remarkable the agreement between the model and the CLAS form factor data for large Q^2 . Except for $A_{3/2}$, the comment holds also for the helicity amplitudes. We recall that the behavior at large Q^2 is a prediction of the model since no parameters are included for the resonance R . The radial wave function associated with the resonance R uses the parameters of the nucleon radial wave function (same momentum distribution).

In both analysis, helicity amplitudes or multipole form factors, the semirelativistic approach deviates from the CLAS data at small Q^2 ($Q^2 < 1.5 \text{ GeV}^2$). Although our calculations are restricted to the limit $M_R = M_N$, we can still assume that the main reason for the deviation between our results and the data for $Q^2 < 1.5 \text{ GeV}^2$ is the consequence of the absence of the meson cloud effects in our formalism, since the meson cloud effects can be very important for some resonances at low Q^2 .

2. Comparison with the EBAC results

We can estimate the contribution for the form factors due to the valence quark or to the meson cloud effects comparing our model with the EBAC estimate of the baryon core effects. The EBAC model is a coupled-channel reaction model that takes into account the meson and photon coupling with the baryon cores. The results presented in the figures are obtained when the meson cloud effects are removed [18, 20]. The EBAC results are represented by the diamonds in the range $Q^2 = 0 - 1.5 \text{ GeV}^2$.

For $A_{1/2}$ and G_M one can see that, the model (solid line) and the EBAC results are very close, particularly near $Q^2 = 1 \text{ GeV}^2$. We can notice also that the EBAC results are closer to our model than the experimental data, in both cases. We then conclude that, the functions $A_{1/2}$ and G_M are dominated by valence quark effects (small meson cloud contributions).

As for $S_{1/2}$ and G_C (proportional functions), we can observe a larger deviation between the model and EBAC, particularly for $Q^2 < 1 \text{ GeV}^2$. The oscillation of the data, and the large errorbars in some cases, invalidates, however, more definitive conclusions.

The results from EBAC for G_E are very interesting, since they are close to our estimate for $Q^2 < 1.5 \text{ GeV}^2$, and also because they are in strong disagreement with the experimental data. This suggests that for G_E (as

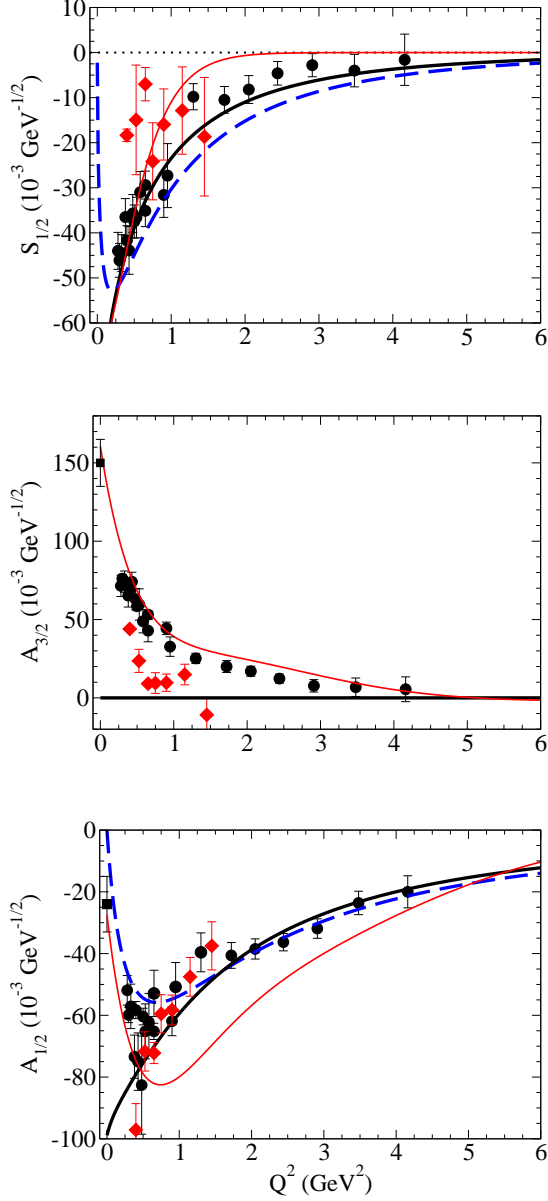


FIG. 1: Results of the $\gamma^* N \rightarrow N(1520)$ helicity amplitudes given by the semirelativistic approximation (thick solid line). Data from PDG [11] (full squares) and CLAS [12–14] (full circles). The thin solid line represent the fit to the MAID data [16]. EBAC estimates from Refs.[18, 19] (diamonds). The *extreme limit* is represented by the dashed line.

for $A_{3/2}$, the contributions of the meson cloud may be significant in order to cover the gap between the results from EBAC and the experimental data. The conclusion that G_E is dominated by meson cloud effects is one of the more important results of the present work. The results for G_E and the connection with $A_{3/2}$ will be discussed in more detail at the end of the section.

In order to study in more detail the result of the approximation $M_R = M_N$, we consider for last, the *extreme limit*, where we take also the $M_R = M_N$ limit in the form

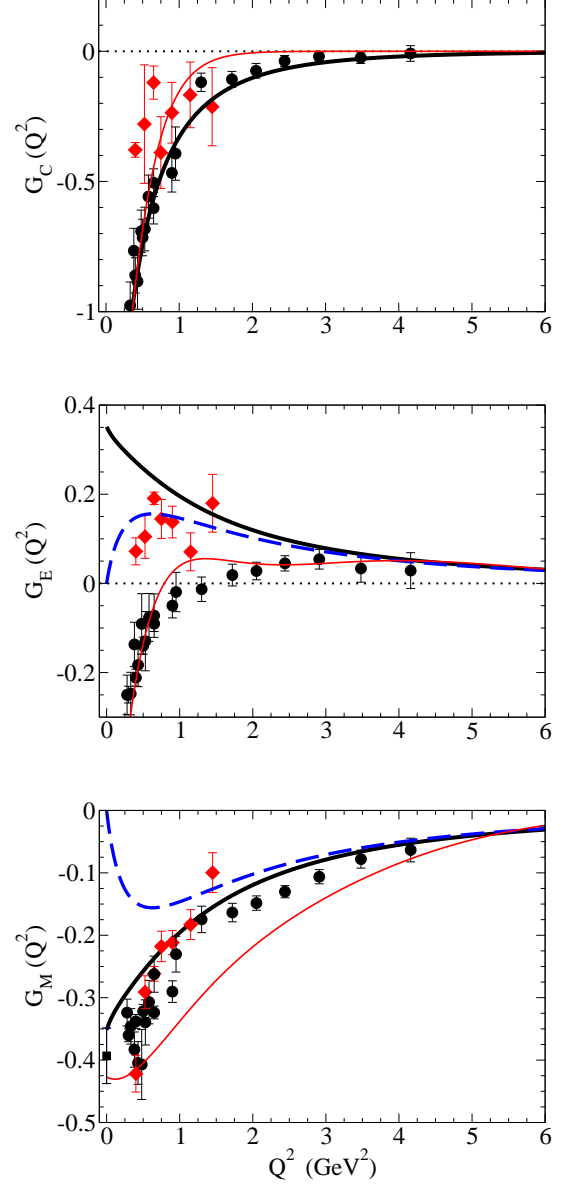


FIG. 2: Results of the $\gamma^* N \rightarrow N(1520)$ form factors given by the semirelativistic approximation (thick solid line). Data from PDG [11] (full squares) and CLAS [12–14] (full circles). The thin solid line represent the fit to the MAID data [16]. EBAC estimates from Refs.[18, 19] (diamonds). The *extreme limit* is represented by the dashed line.

factors coefficients of Eqs. (3.11)-(3.13) and Eqs. (3.14)-(3.16). The results are present in Figs. 1 and 2 by the dashed line. In that case we use $Q_-^2 = Q^2$, and replace also $|\mathbf{q}| \rightarrow Q\sqrt{1+\tau}$ in $S_{1/2}$. As a consequence of the *extreme limit*, the functions $A_{1/2}$, $S_{1/2}$, G_E and G_M vanish at $Q^2 = 0$. The form factor G_C does not vanish at $Q^2 = 0$, because the factor $|\mathbf{q}|$ cancels the $Q \rightarrow 0$ dependence of $S_{1/2}$ (since $G_C \propto S_{1/2}/|\mathbf{q}|$). Although the *extreme limit* spoils the semirelativistic approximation from the nice features discussed before (finite result at $Q^2 = 0$ for amplitudes and form factors) it is still interesting to

note that the model is close to the CLAS data at low Q^2 ($A_{1/2}, S_{1/2}$) or close to EBAC (G_E).

B. $\gamma^* N \rightarrow N(1535)$ transition

We present now the results of the semirelativistic approximation for the $\gamma^* N \rightarrow N(1535)$ transition. We start with the discussion of the transition form factors, later we discuss the helicity amplitudes.

The available data for the $A_{1/2}$ and $S_{1/2}$ amplitudes covers the region $Q^2 = 0 - 4.2 \text{ GeV}^2$ [11, 12, 15, 16]. The large Q^2 data for $A_{1/2}$ comes from the Ref. [17] with $Q^2 = 5.8, 7.0 \text{ GeV}^2$, and was extracted under the assumption that the $S_{1/2}$ contribution for the cross section is negligible. Therefore in the conversion from helicity amplitudes to transition form factors we use $S_{1/2} = 0$.

In Ref. [29] was suggested that in the region $Q^2 > 2 \text{ GeV}^2$ the amplitudes are related by $S_{1/2} = -\frac{\sqrt{1+\tau}}{\sqrt{2}} \frac{M_R^2 - M_N^2}{2M_R Q} A_{1/2}$. One can then use the relation to estimate the expected value for $S_{1/2}$ according to the values $A_{1/2}$ from Ref. [17] for large Q^2 . In the following we use the solid triangles for the original result ($S_{1/2} = 0$) and the empty triangles for the asymptotic estimate.

1. Form factors

We start with the $\gamma^* N \rightarrow N(1535)$ results for the form factors F_1^* and F_2^* . In the calculation of the overlap integral $\mathcal{I}_R(Q^2)$, we use the replacement of $M_R, M_N \rightarrow M$. In the calculation of the form factors we consider in addition the replacement $\frac{M_R + M_N}{2M_N} \rightarrow 1$, in the expression for F_2^* . In the semirelativistic approach, since $F_i^*(Q^2) \propto \mathcal{I}_R(Q^2)$ and $\mathcal{I}_R(0) = 0$, one has $F_1^*(0) = 0$, and $F_2^*(0) = 0$. The first result is consistent with the data (by construction). The second result is an approximation of our model, since the experimental value is $F_2^*(0) = 0.83 \pm 0.28$ [11].

The results for the form factors are presented in Fig. 3 and are compared with the data from CLAS, MAID and JLab/Hall C [12, 15–17] for $Q^2 > 0$.

In the Fig. 3, one can note for F_1^* , the good agreement between the model (solid line) and the data (CLAS and MAID) for $Q^2 > 2 \text{ GeV}^2$. As for F_2^* , we conclude as in the previous work [8] that the model predictions for F_2^* are not in agreement with the data (difference of sign between the model and the data).

Our interpretation is that in the case of F_2^* it is possible that the meson cloud effects may be significant. Since we did not include the meson cloud effects, the model deviates from the F_2^* data. Our hypothesis is corroborated by the EBAC estimate of the bare core, represent in the graphs by the diamond and also by explicit calculations of meson cloud effects based in the unitary chiral model, where the baryons states are represented by bare cores dressed by mesons [30, 49]. In the graph for F_1^* we can

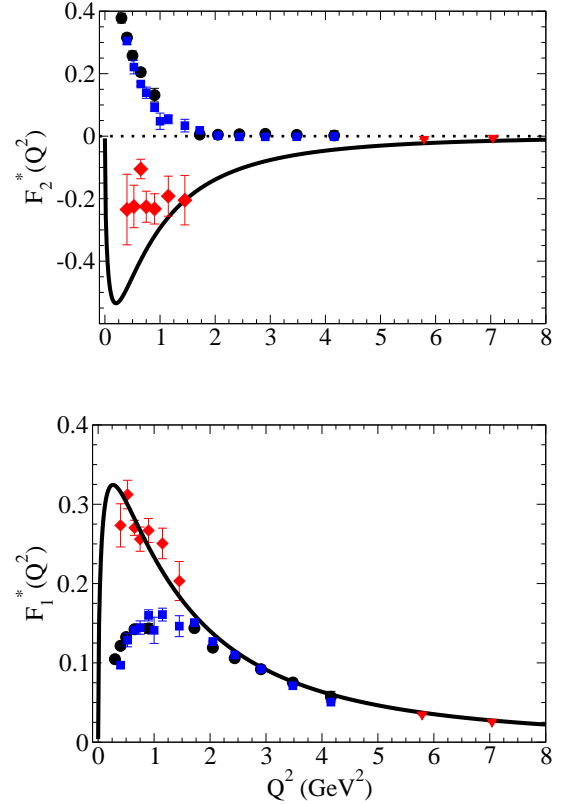


FIG. 3: Results for the $\gamma^* N \rightarrow N(1535)$ transition form factors given by the semirelativistic approximation (thick solid line). Data from CLAS [12] (full circles), MAID [15, 16] (full squares), JLab/Hall C [17] (triangles). EBAC results from [18, 19] (diamond). Out of the range is the PDG result $F_2^*(0) = 0.83 \pm 0.28$ [11].

note the excellent agreement between our model and the EBAC result. Our results for F_1^* are impressive, since they describe, simultaneously, the experimental data for $Q^2 > 2 \text{ GeV}^2$, and the EBAC estimate of the bare core for $Q^2 < 2 \text{ GeV}^2$.

2. Helicity amplitudes

In the case of the $\gamma^* N \rightarrow N(1535)$ transition there is no simple procedure to calculate the helicity amplitudes using our results in the semirelativistic approximation (limit $M_R = M_N$), since in the calculation of the helicity amplitudes (3.18) and (3.19) the mass difference is crucial. If we use $M_R = M_N$ in $A_{1/2}$, we suppress the contribution from F_2^* , and $A_{1/2}$ is determined exclusively by F_1^* . If we use $M_R = M_N$ in $S_{1/2}$, we remove the effect of F_1^* , the more relevant form factor.

Our first conclusion then is that the semirelativistic approximation to the $\gamma^* N \rightarrow N(1535)$ transition is better for the form factors than for the helicity amplitudes.

To compare our estimates in the semirelativistic approach we need to consider additional simplifications. We

consider the two following cases:

- **Model A** (or valence quark model)

It is defined by the semirelativistic approach to the form factors with no further constraints. Since no explicit meson cloud effects are included, the model is expected to fail the description of the data at low Q^2 . It may happen, however, that the model is comparable with the results from EBAC.

- **Model B** (or high Q^2 model)

It is defined by the condition $F_2^* = 0$, combined with the result of the model for F_1^* . Since the result $F_2^* = 0$ holds only for high Q^2 , the model is expected to be good only for large values of Q^2 .

In both cases we use the original definition of amplitudes (3.18) and (3.19). In the analysis we discuss also the effect of the replacement $|\mathbf{q}| \rightarrow Q\sqrt{1+\tau}$ in the amplitude $S_{1/2}$ given by Eq. (3.19). With the previous correction, $S_{1/2}$ became

$$S_{1/2} = \sqrt{2}A_R(M_R + M_N)(1 + \tau) \times \left[\frac{M_R - M_N}{M_R + M_N} \frac{F_1^*}{|\mathbf{q}|} - \tau \frac{F_2^*}{|\mathbf{q}|} \right], \quad (5.4)$$

where $\frac{F_i^*}{|\mathbf{q}|}$ ($i = 1, 2$) are well defined functions at $Q^2 = 0$, as discussed already. With the form (5.4) the divergence in $1/Q^2$ of $S_{1/2}$ is avoided and $S_{1/2}(0)$ became finite.

The results for the amplitudes are presented in Fig. 4 for the model A and in Fig. 5 for the model B. In the figures, we include the data from Ref. [17] for $Q^2 > 5$ GeV². In the case of $S_{1/2}$ we include also the estimate from Ref. [29], as discussed earlier (empty triangles). In the graphs for $S_{1/2}$ the thick lines represent the original result for the amplitude, given by Eq. (3.19) and the thin line the redefinition (5.4). In the last case, $S_{1/2}(0)$ is finite although it is not shown in the graph.

In Fig. 4, we compare the valence quark model (model A) with the physical data (PDG, CLAS, MAID and JLab/Hall C) and also with the results from EBAC. Note for $S_{1/2}$, the close agreement with EBAC (region $Q^2 < 1.5$ GeV²) in both descriptions (thick and thin lines). The deviation from the physical data is an indication of the strong meson cloud effect expected for this amplitude. As for the amplitude $A_{1/2}$ it may be a surprise to see that the model is closer to the physical data than from EBAC, since the results for the form factors are more comparable with EBAC than with the data (see Fig. 3). This effect is a consequence of the small overestimation of the model for the form factor F_2^* combined with the difference of sign between F_1^* and the F_2^* in the calculation of $A_{1/2}$ given by Eq. (3.18). The closeness between the model A and the $A_{1/2}$ data for small Q^2 may be interpreted as a coincidence due to the results observed for the form factors (the model cannot describe simultaneously the form factors F_1^* , F_2^* in the region $Q^2 < 2$ GeV²). As for large Q^2 the closeness between model and

data is expectable due the predicted falloff of the meson cloud contributions, and also due to the smaller impact of F_2^* in $A_{1/2}$ [see Eq. (3.18)].

The model A can be very useful in the future to compare with lattice QCD simulations at large pion masses (no meson cloud effects). In future works one may use the difference between our estimate of the bare core and a parametrization of the data to extract the effects of the meson cloud.

In Fig. 5, we compare the high Q^2 model (model B) directly with the data. Since the result $F_2^* = 0$ is observed only for $Q^2 > 1.5$ GeV², we represent the lines differently below (dotted line) and above (solid line) that point. For $Q^2 > 1.5$ GeV² it is clear the agreement between the model and the physical data (CLAS, MAID and JLab/Hall C) for both amplitudes. In the graph for $S_{1/2}$ the results from Eq. (3.19), which diverge at $Q^2 = 0$ (thick line), are closer to the data than the result from Eq. (5.4) (thin line), and are finite at $Q^2 = 0$. Both results are however at the range of about 1.5 standard deviations in the region of interest ($Q^2 > 1.5$ GeV²).

The closeness between the model B and the data for $Q^2 > 1.5$ GeV² is very interesting and claims for additional experimental studies in order to test the hypothesis $F_2^* = 0$ in more detail. Also noticeable is the agreement between the model and the estimate of the $S_{1/2}$ amplitude from Ref. [29] (empty triangles) using the data from JLab/Hall C [17]. To clarify this point, new data or a reanalysis of old data using the Rosenbluth separation method (that allows the separation of different components of the measured cross section) would be very welcome.

C. Discussion

Using the semirelativistic approximation we improved the results from the covariant spectator quark model from Refs. [8, 9]. The orthogonality between states is ensured and we obtain now analytic results consistent with the low Q^2 data. In particular we predict non-zero results for $A_{1/2}, G_M, G_E$ for $Q^2 = 0$ in the $\gamma^*N \rightarrow N(1520)$ transition and still preserve the result $F_1^*(0) = 0$ for the $\gamma^*N \rightarrow N(1535)$ transition.

Comparative to the models from Ref. [8, 9], where the estimate of the valence quark contributions for the form factors were good only for large Q^2 , we present more reliable estimates for the low Q^2 region, although derived under the assumption that $M_R \simeq M_N$. A more accurate estimate of the valence quark contributions in the low Q^2 regime is very important, since the parametrization can be used to estimate the meson cloud effects based on a parametrization of the form factors data. A parametrization of the valence quark contributions can also be very useful to compare with lattice simulations with large pion masses (suppression of meson cloud effects).

Our results for the $\gamma^*N \rightarrow N(1520)$ are in good agreement with the large Q^2 data ($Q^2 > 3$ GeV²) and with the

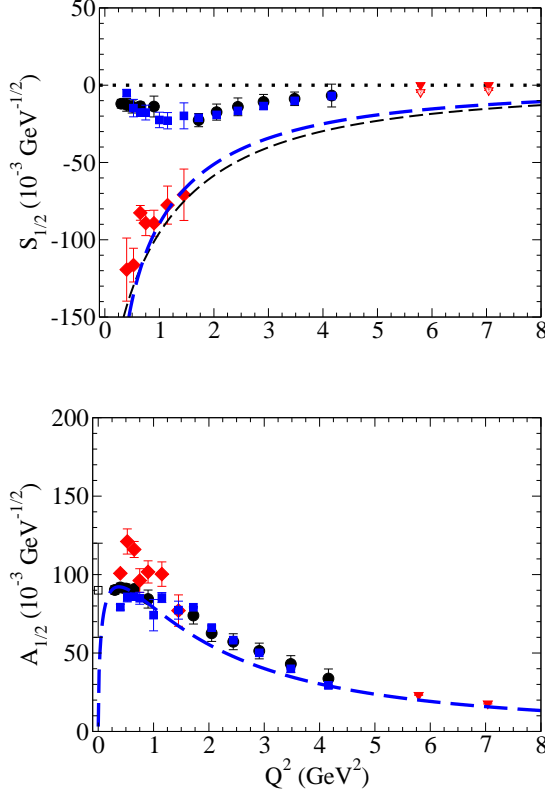


FIG. 4: Results for the $\gamma^*N \rightarrow N(1535)$ helicity amplitudes given by the model A (dashed line). Estimate of the valence quark contributions. Data from PDG (empty square) [11], CLAS [12] (full circles), MAID [15, 16] (full squares), JLab/Hall C [17] (triangles). EBAC results from [18, 19] (diamond).

EBAC results at low Q^2 ($Q^2 < 1.5 \text{ GeV}^2$). The exception is the amplitude $A_{3/2}$ for which the spectator quark model predicts zero contributions.

The experimental results (with meson cloud) and the EBAC results for the bare core (no meson cloud) for G_E can be understood in the case where $A_{3/2}$ is mainly a consequence of the meson cloud effects and $A_{1/2}$ is dominated by valence quark effects (small meson cloud contributions). The relations between the meson cloud (index mc) contributions from the helicity amplitudes and form factors can be represented as [1, 9]

$$A_{1/2}^{\text{mc}} = \frac{1}{4F}(3G_M^{\text{mc}} - G_E^{\text{mc}}) \quad (5.5)$$

$$A_{3/2}^{\text{mc}} = -\frac{\sqrt{3}}{4F}(G_M^{\text{mc}} + G_E^{\text{mc}}), \quad (5.6)$$

where F is a given function of Q^2 [9]. When $|A_{3/2}^{\text{mc}}| \gg |A_{1/2}^{\text{mc}}|$, we can conclude that

$$G_E^{\text{mc}} = -\frac{F}{\sqrt{3}}A_{3/2}^{\text{mc}}, \quad G_M^{\text{mc}} = \frac{1}{3}G_E^{\text{mc}}. \quad (5.7)$$

Thus, in the case where the meson cloud contributions are large for $A_{3/2}$ and small for $A_{1/2}$, G_E has larger meson cloud contributions, proportional to $A_{3/2}^{\text{mc}}$, and G_M

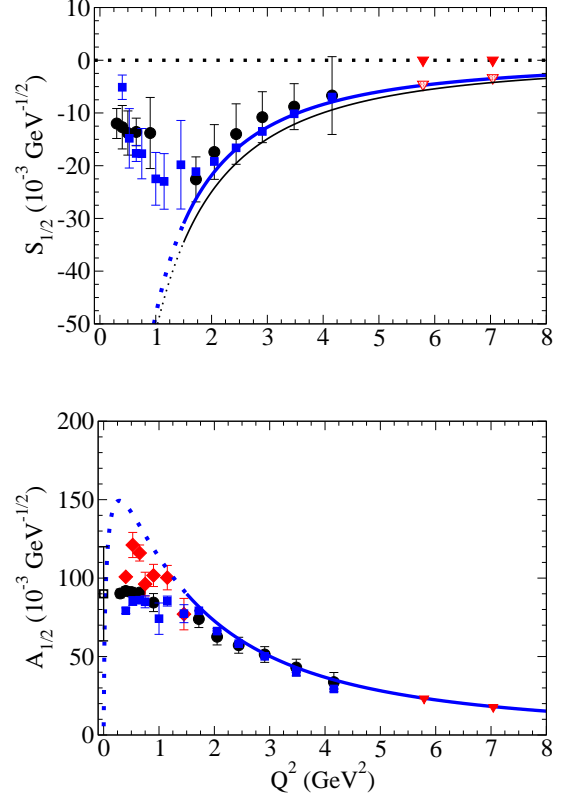


FIG. 5: Results for the $\gamma^*N \rightarrow N(1535)$ helicity amplitudes given by the model B (dashed line). Estimate valid for large Q^2 . Data from PDG (empty squares) [11], CLAS [12] (full circles), MAID [15, 16] (full squares), Jlab/Hall C [17] (triangles). EBAC results from [18, 19] (diamond).

has smaller meson cloud contributions (about one third of the contribution for G_E). Those results are compatible with the results of Figs. 1 and 2 for $A_{1/2}$ and G_M . We note also that the dominance of the meson cloud effects in the amplitude $A_{3/2}$ was already observed in the EBAC model [18]. Indications of the the large meson cloud contributions for $A_{3/2}$ came also from quark models where the valence quark contributions are only about a small fraction of the experimental values [50–53].

Our results for the $\gamma^*N \rightarrow N(1535)$ form factors are compatible with the results from EBAC (bare core contribution) when $Q^2 < 1.5 \text{ GeV}^2$, and differs from the experimental data. We can interpret those results as a manifestation of the absence of meson cloud effects, particularly for F_2^* . For the $\gamma^*N \rightarrow N(1535)$ transition the semirelativistic approximation with $M_R = M_N$ is unapropriated for the calculation of the helicity amplitudes. For the $\gamma^*N \rightarrow N(1535)$ transition, one can use, however, two simple approximations: one based on the valence quark contributions (model A), another that is valid for large Q^2 , and compares well with the data (model B with $F_2^* = 0$).

Overall, we conclude that we have a good description of the valence quark content of the $N(1520)$ and $N(1525)$

systems, since we describe the large Q^2 data and the results from EBAC (bare core).

VI. OUTLOOK AND CONCLUSIONS

In this work we present a new method to calculate the $\gamma^*N \rightarrow R$ transition form factors, where R is a negative parity resonance within the covariant spectator quark model. We call the method the semirelativistic approximation. The semirelativistic approximation is defined by taking the limit $M_R = M_N$ in the overlap integral between the radial wave functions.

In the semirelativistic approximation the proprieties of the nonrelativistic limit of the states, in particular the orthogonality between those wave functions and the nucleon wave function, are preserved, but the formalism is still covariant. The wave functions of the R states are defined using the same parametrization for the radial wave functions as for the nucleon.

We use analytic results from previous works and apply the semirelativistic approximation to the cases $R = N(1520)$, $N(1535)$. Within the approximation we calculate the valence quark contributions for the transition form factors and helicity amplitudes. Since the wave functions of those states are defined in terms of the parametrization to the nucleon, the calculations provide true predictions for the transition form factors and helicity amplitudes.

In general, our estimates are based exclusively on the valence quark degrees of freedom are in excellent agreement with the results for the form factors for $Q^2 > 3 \text{ GeV}^2$ and with the EBAC estimates of the baryon core at low Q^2 (when the meson cloud is removed). We then conclude that we have a good description of valence quark content of the nucleon, $N(1520)$ and $N(1535)$ systems. Our valence quark parametrization can in principle be tested in the future by lattice QCD simulations.

The semirelativistic approximation is more appropriated for the form factors than for the helicity amplitudes.

The calculation of the helicity amplitudes must be done with some care, since it depends critically of the mass difference, particularly in the $\gamma^*N \rightarrow N(1535)$ case. For the $\gamma^*N \rightarrow N(1520)$ transition we obtained has a good description of the helicity amplitudes for $Q^2 > 3 \text{ GeV}^2$. The amplitude $A_{3/2}$ is the exception, since this amplitude is expected to be dominated by meson cloud effects. As for the $\gamma^*N \rightarrow N(1535)$ transition, we present a parametrization of the amplitudes for large Q^2 .

From our study, we can conclude that the $N(1520)$ and $N(1535)$ resonances are very interesting physical systems. The transition form factors associated with the $N(1520)$ and $N(1535)$ are in general dominated by the valence quark effects with a few exceptions. The electric form factor G_E in the $\gamma^*N \rightarrow N(1520)$ transition which is strongly dominated by meson cloud contributions. There is also evidences that the form factor F_2^* in the $\gamma^*N \rightarrow N(1535)$ transition, as discussed already in the literature.

To summarize, we present parametrizations for the $\gamma^*N \rightarrow N(1520)$ and $\gamma^*N \rightarrow N(1535)$ transition form factors and respective helicity amplitudes, that are consistent with the available data in the regime of $Q^2 = 3\text{--}7 \text{ GeV}^2$. Our predictions may be tested in the future JLab 12-GeV upgrade up to 12 GeV^2 [54]. Of particular interest is the test of our high Q^2 model for the $\gamma^*N \rightarrow N(1535)$ transition (with $F_2^* = 0$) which predicts the relation between amplitudes $S_{1/2} = -\frac{\sqrt{1+\tau}}{\sqrt{2}} \frac{M_R^2 - M_N^2}{2M_R Q} A_{1/2}$ [29] and was till the moment tested only up to $Q^2 = 4.2 \text{ GeV}^2$, by the CLAS and MAID data [12, 15, 16].

Acknowledgments

The author thanks Hiroyuki Kamano for providing the EBAC results from Refs. [18, 19]. This work was supported by the Brazilian Ministry of Science, Technology and Innovation (MCTI-Brazil).

-
- [1] I. G. Aznauryan and V. D. Burkert, Prog. Part. Nucl. Phys. **67**, 1 (2012) [arXiv:1109.1720 [hep-ph]].
 - [2] I. G. Aznauryan, A. Bashir, V. Braun, S. J. Brodsky, V. D. Burkert, L. Chang, C. Chen and B. El-Bennich *et al.*, Int. J. Mod. Phys. E, **22**, 1330015 (2013) [arXiv:1212.4891 [nucl-th]].
 - [3] S. Capstick and W. Roberts, Prog. Part. Nucl. Phys. **45**, S241 (2000) [nucl-th/0008028].
 - [4] N. Isgur and G. Karl, Phys. Rev. D **19**, 2653 (1979) [Erratum-ibid. D **23**, 817 (1981)]; R. Koniuk and N. Isgur, Phys. Rev. D **21**, 1868 (1980) [Erratum-ibid. D **23**, 818 (1981)].
 - [5] S. Capstick and B. D. Keister, Phys. Rev. D **51**, 3598 (1995) [nucl-th/9411016].
 - [6] I. G. Aznauryan, Phys. Rev. C **76**, 025212 (2007) [arXiv:nucl-th/0701012].
 - [7] I. G. Aznauryan and V. D. Burkert, Phys. Rev. C **85**, 055202 (2012) [arXiv:1201.5759 [hep-ph]].
 - [8] G. Ramalho and M. T. Peña, Phys. Rev. D **84**, 033007 (2011) [arXiv:1105.2223 [hep-ph]].
 - [9] G. Ramalho and M. T. Peña, arXiv:1610.08788 [nucl-th]; G. Ramalho and M. T. Peña, Phys. Rev. D **89**, 094016 (2014) [arXiv:1309.0730 [hep-ph]].
 - [10] G. Ramalho, Phys. Rev. D **90**, 033010 (2014) [arXiv:1407.0649 [hep-ph]].
 - [11] J. Beringer *et al.* [Particle Data Group Collaboration], Phys. Rev. D **86**, 010001 (2012).
 - [12] I. G. Aznauryan *et al.* [CLAS Collaboration], Phys. Rev. C **80**, 055203 (2009) [arXiv:0909.2349 [nucl-ex]].
 - [13] V. I. Mokeev *et al.* [CLAS Collaboration], Phys. Rev. C **86**, 035203 (2012) [arXiv:1205.3948 [nucl-ex]].
 - [14] V. I. Mokeev *et al.*, Phys. Rev. C **93**, 025206 (2016)

- [arXiv:1509.05460 [nucl-ex]].
- [15] D. Drechsel, S. S. Kamalov and L. Tiator, Eur. Phys. J. A **34**, 69 (2007) [arXiv:0710.0306 [nucl-th]].
- [16] L. Tiator, D. Drechsel, S. S. Kamalov and M. Vanderhaeghen, Chin. Phys. C **33**, 1069 (2009) [arXiv:0909.2335 [nucl-th]].
- [17] M. M. Dalton *et al.*, Phys. Rev. C **80**, 015205 (2009) [arXiv:0804.3509 [hep-ex]].
- [18] B. Julia-Diaz, H. Kamano, T. S. H. Lee, A. Matsuyama, T. Sato and N. Suzuki, Phys. Rev. C **80**, 025207 (2009). [arXiv:0904.1918 [nucl-th]].
- [19] H. Kamano, private communication. The EBAC amplitudes $A_{1/2}$ and $A_{3/2}$ differ from the other analysis by a sign. Amplitudes converted to the PDG convention.
- [20] T. Sato and T. -S. H. Lee, J. Phys. G **36**, 073001 (2009) [arXiv:0902.3653 [nucl-th]].
- [21] L. Tiator, D. Drechsel, S. Kamalov, M. M. Giannini, E. Santopinto and A. Vassallo, Eur. Phys. J. A **19**, 55 (2004) [nucl-th/0310041].
- [22] F. Gross, G. Ramalho and M. T. Peña, Phys. Rev. C **77**, 015202 (2008) [nucl-th/0606029].
- [23] F. Gross, G. Ramalho and M. T. Peña, Phys. Rev. D **85**, 093005 (2012) [arXiv:1201.6336 [hep-ph]].
- [24] G. Ramalho, K. Tsushima and F. Gross, Phys. Rev. D **80**, 033004 (2009) [arXiv:0907.1060 [hep-ph]].
- [25] G. Ramalho and K. Tsushima, Phys. Rev. D **89**, 073010 (2014) [arXiv:1402.3234 [hep-ph]].
- [26] G. Ramalho, M. T. Peña and F. Gross, Phys. Rev. D **78**, 114017 (2008) [arXiv:0810.4126 [hep-ph]].
- [27] G. Ramalho and K. Tsushima, Phys. Rev. D **81** (2010) 074020 [arXiv:1002.3386 [hep-ph]].
- [28] G. Ramalho, Phys. Rev. D **93**, 113012 (2016) [arXiv:1602.03832 [hep-ph]].
- [29] G. Ramalho and K. Tsushima, Phys. Rev. D **84**, 051301 (2011) [arXiv:1105.2484 [hep-ph]].
- [30] G. Ramalho, D. Jido and K. Tsushima, Phys. Rev. D **85**, 093014 (2012) [arXiv:1202.2299 [hep-ph]].
- [31] G. Ramalho, Phys. Lett. B **759**, 126 (2016) [arXiv:1602.03444 [hep-ph]].
- [32] Comparative to the Refs. [8, 29] the form factors are corrected by a sign.
- [33] F. Gross, Phys. Rev. **186**, 1448 (1969); A. Stadler, F. Gross and M. Frank, Phys. Rev. C **56**, 2396 (1997). [arXiv:nucl-th/9703043].
- [34] G. Ramalho, M. T. Peña and F. Gross, Eur. Phys. J. A **36**, 329 (2008) [arXiv:0803.3034 [hep-ph]].
- [35] G. Ramalho and M. T. Peña, Phys. Rev. D **80** (2009) 013008 [arXiv:0901.4310 [hep-ph]].
- [36] F. Gross, G. Ramalho and M. T. Peña, Phys. Rev. D **85**, 093006 (2012) [arXiv:1201.6337 [hep-ph]].
- [37] F. Gross, G. Ramalho and M. T. Peña, Phys. Rev. C **77**, 035203 (2008).
- [38] G. Ramalho, M. T. Peña and F. Gross, Phys. Rev. D **81**, 113011 (2010) [arXiv:1002.4170 [hep-ph]]; G. Ramalho and M. T. Peña, Phys. Rev. D **85**, 113014 (2012) [arXiv:1205.2575 [hep-ph]]; G. Ramalho, M. T. Peña, J. Weil, H. van Hees and U. Mosel, Phys. Rev. D **93**, 033004 (2016) [arXiv:1512.03764 [hep-ph]].
- [39] G. Ramalho, M. T. Peña and A. Stadler, Phys. Rev. D **86**, 093022 (2012) [arXiv:1207.4392 [nucl-th]].
- [40] G. Ramalho and M. T. Peña, J. Phys. G **36**, 115011 (2009) [arXiv:0812.0187 [hep-ph]].
- [41] G. Ramalho and K. Tsushima, Phys. Rev. D **82**, 073007 (2010) [arXiv:1008.3822 [hep-ph]].
- [42] G. Ramalho and K. Tsushima, Phys. Rev. D **84**, 054014 (2011) [arXiv:1107.1791 [hep-ph]]; G. Ramalho and K. Tsushima, Phys. Rev. D **86**, 114030 (2012) [arXiv:1210.7465 [hep-ph]]; G. Ramalho, K. Tsushima and A. W. Thomas, J. Phys. G **40**, 015102 (2013) [arXiv:1206.2207 [hep-ph]].
- [43] G. Ramalho and K. Tsushima, Phys. Rev. D **88**, 053002 (2013) [arXiv:1307.6840 [hep-ph]]; G. Ramalho and K. Tsushima, Phys. Rev. D **87**, 093011 (2013) [arXiv:1302.6889 [hep-ph]].
- [44] G. Ramalho and M. T. Peña, Phys. Rev. D **83**, 054011 (2011) [arXiv:1012.2168 [hep-ph]].
- [45] J. J. Kelly, Phys. Rev. C **56**, 2672 (1997).
- [46] Z. Batiz and F. Gross, Phys. Rev. C **58**, 2963 (1998) [arXiv:nucl-th/9803053].
- [47] R. A. Gilman and F. Gross, J. Phys. G **28**, R37 (2002) [nucl-th/0111015].
- [48] V. D. Burkert, R. De Vita, M. Battaglieri, M. Ripani and V. Mokeev, Phys. Rev. C **67**, 035204 (2003) [hep-ph/0212108].
- [49] D. Jido, M. Döring and E. Oset, Phys. Rev. C **77**, 065207 (2008).
- [50] M. Aiello, M. M. Giannini and E. Santopinto, J. Phys. G **24**, 753 (1998) [nucl-th/9801013].
- [51] T. Melde, W. Plessas and B. Sengl, Phys. Rev. D **77**, 114002 (2008) [arXiv:0806.1454 [hep-ph]].
- [52] E. Santopinto and M. M. Giannini, Phys. Rev. C **86**, 065202 (2012) [arXiv:1506.01207 [nucl-th]].
- [53] M. Ronniger and B. C. Metsch, Eur. Phys. J. A **49**, 8 (2013) [Eur. Phys. J. A **49**, 8 (2013)] [arXiv:1207.2640 [hep-ph]].
- [54] I. Aznauryan, V. Braun, V. Burkert, S. Capstick, R. Edwards, I. C. Cloet, M. Giannini and T. S. H. Lee *et al.*, arXiv:0907.1901 [nucl-th].